2008 10th Intl. Conf. on Control, Automation, Robotics and Vision
Hanoi, Vietnam, 17–20 December 2008

Dynamics Analysis of A Redundant Parallel Manipulator Driven By Elastic Cables

Y. Babazadeh Bedoustani, H. D. Taghirad and M. M. Aref
Department of Electrical Engineering, K.N. Toosi University of Technology
Advance Robotics and Automated Systems (ARAS)
Tehran, Iran
yousef_babazadeh@ee.kntu.ac.ir

***Abstract*— In this paper the dynamic analysis of a cable-driven parallel manipulator is studied in detail. The manipulator architecture is a simplified planar version adopted from the structure of Large Adaptive Reflector (LAR), the Canadian design of next generation giant radio telescopes. This structure consists of a parallel redundant manipulator actuated by long cables. The dynamic equations of this structure are nonlinear and implicit. Long cables, large amounts of impelling forces and high accelerations raise more concern about the elasticity of cables during dynamic analysis, which has been neglected in the preceding works. In this paper, the kinematic analysis of such manipulator is illustrated first. Then the nonlinear dynamic of such mechanism is derived using Newton-Euler formulation. Next a simple model for cable dynamics containing elastic and damping behavior is proposed. The proposed model neither ignores longitude elasticity properties of cable nor makes dynamic formulations heavily complicated like previous researches. Finally, manipulator dynamic with cable dynamic is derived, and the cable elasticity effects are compared in a simulation study. The results show significant role of elasticity in a cable-driven parallel manipulator such as the one used in LAR mechanism.**

***Keywords*—Cable-Driven Parallel Manipulator, Elastic Cable, Kinematics, Dynamics, Redundant Manipolator**

I. INTRODUCTION

An international consortium of radio astronomers and engineers have agreed to investigate technologies to build the Square Kilometer Array (SKA), a cm-to-m wave radio telescope for the next generation of investigation into cosmic phenomena [1]. The Canadian proposal for the SKA design consists of an array of 30-50 individual antennas whose signals are combined to yield the resolution of a much larger antenna. Each of these antennas would use the Large Adaptive Reflector (LAR) concept put forward by a group led by the National Research Council of Canada and supported by university and industry collaborators [2]. Design and construction of a 200-m LAR prototype is pursued by the National Research Council of Canada. Figure 1 is an artist's concept of a complete 200-m diameter LAR installation, which consists of two central components. The first is a 200 m diameter parabolic reflector and the second component is the receiver package which is supported by a tension structure consisting of multiple long tethers and a helium filled aerostat. A one-third scale prototype of the multi-tethered aerostat subsystem [3] has been designed and implemented in Penticton. The challenging problem in this

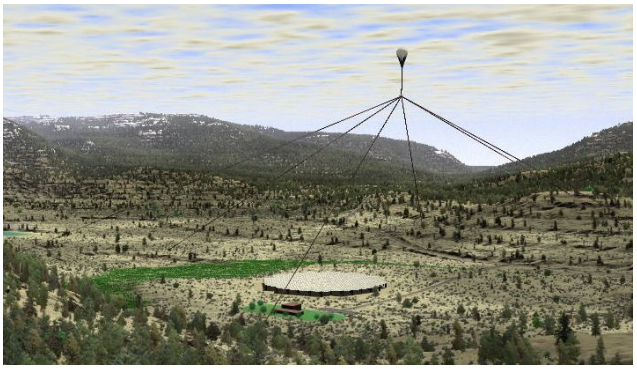

Fig. 1. An artist's concept of LAR installation

positioning structure of the receiver a redundantly actuated cable-driven parallel manipulators is used [4]. In which, the receiver is moved to various locations on a circular hemisphere and its positioning is controlled by changing the lengths of eight tethers with ground winches. The cable driven redundant manipulator used in this design, which is called the Large Cable Mechanism (LCM), is in fact a 6DOF cable driven redundant manipulator. In the design of LCM a redundantly actuated parallel manipulator is used for extreme positioning accuracy. This structure is composed of a 4RPR mechanisms actuated by cables. In this simplified structure, although a planar version of the mechanisms are considered. The important feature of the original design namely the actuator redundancy for each subsystem and the cable driven structure of the original design are employed. In contrast to the open-loop kinematic chain serial manipulators, the dynamic modeling of parallel manipulators presents an inherent complexity due to their closed-loop kinematic chain structure and kinematic constraints. Nevertheless, the dynamic analysis is quite important for their design and control. There are numerous works have been done in cable driven manipulator's dynamic analysis. However, cables elasticity effects are neglected by some researches on dynamic analysis of cable-driven parallel manipulators [5], while they are using light weight end-effectors, small workspace, which leads to use short cables. Such modeling of dynamic has less concern about elastic effects on the manipulator's dynamic when used in low accelerations. However, in the other works elasticity of cables are also ignored even in a wide workspace with a heavy end-effector [4][6]. In a heavy loaded cable-driven manipulator

like LCM cable dynamic has a significant role in the dynamics of the whole system. In view of cable capability of transmitting forces and carrying payloads, the cable modeling is a basic element of theoretical interest in applied mechanics and dynamics. The great diversity of cable applications has led to different elastic cable theories. In one of the intensive works, nonlinear vibrations of suspended cable have been studied by Giuseppe Rega [7],[8]. In a real situation, cable dynamics is considered as a continuous or distributed parameter system. Therefore, cable dynamic behavior described by a second-order partial differential equation is not easily solvable when external forces are applied. To simplify the analysis, the cables are modeled using a lumped-mass discretization approach, which leads to a series of equations of motion that are solvable using standard numerical integration techniques [9]. The reliability of lumped-mass cable models for predicting the dynamic behavior of long cables has been previously verified through experimental validation of marine systems [10],[11].

This paper is intended to study the kinematic and dynamic analysis of such structures in detail. In kinematic analysis the joint space variables and the manipulator Jacobian are obtained while cables are assumed lumped-mass. Dynamic behavior of manipulator is analyzed using the traditional Newton–Euler formulation. Then, a simplified linear elastic model of cable is proposed to determine cable dynamics. For this purpose, it is assumed that the cable is consisted of only one lumped-mass and the cable elasticity and damping effect is considered as a spring-dashpot collected on one side of this lumped body. With this assumption, a simplified model that contains the cable elastic and damping behavior is generated. Including this cable model into the overall manipulator dynamics, significant influence in the dynamic behavior of manipulator is observed, while avoiding complicated processes for elasticity modeling. Due to implicit nature of the dynamic equations, usual numerical integration routines such as Runge–Kutta methods, cannot be used to solve this problem [9]. The dynamic equations of the system are used in two sets of simulations. The inverse dynamic simulations are presented first, in which the required actuator torques required to generate a predefined trajectory is computed. Finally, forward dynamics simulations is performed, which show that the elasticity in cable has an important effect on manipulator's end-effector positioning performance.

II. Mecanism and Kinematic Analysis

The planar structure used in this analysis, is a simplified version of LCM design. The control objective in the simplified

TABLE I. Geometric And Inertial Parameters of The System

Description	Symbols	Quantity
Radius of location circle of fixed points Ai's	R_A	900 m
Radius of location circle of moving platform points Bi's	R_B	10 m
Angle of fixed points Ai's	Θ_A	[-135°,-45°,45°,135°]
Angle of moving attachment platform points Bi's	Θ_B	[-45°,-135°,135°,45°]
The moving platform's mass	M	2500 kg
The moving platform'smoments of inertia	I_M	3.5e5 kg/m
The limb density per length	ρ_M	0.215 kg/m

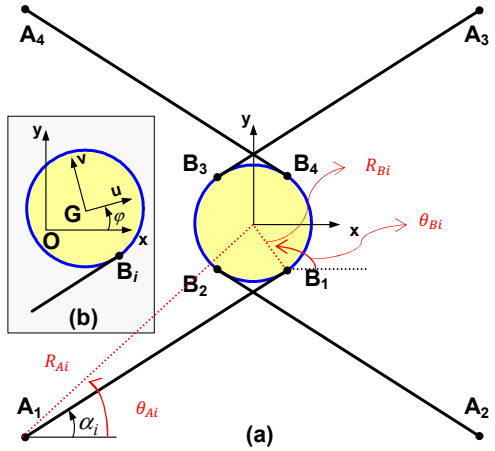

Fig. 2. 4RPR mechanism used as parallel manipulator for LCM structure.

mechanism is to track the position and orientation of the moving platform as desired in presence of disturbance force, such as wind turbulence. The geometric and inertial parameters used in the simulations of the system is adopted from LCM design and is given in *Table I*, in which M and I denote the mass and the moment of inertia of the moving platform, respectively, ρ_M denotes the limb density per length.

The architecture of the planar 4RPR parallel manipulator considered for our work is shown in figure 2(a). In this manipulator the moving platform is supported by four limbs of identical kinematic structure. Each limb connects the fixed base to the manipulator moving platform by a revolute joint (R) followed by a prismatic joint (P) and another revolute joint (R). In this way as shown in figure 2(a) we have one revolute joint at point A_i, a prismatic joint along cable length and also a revolute joint at point B_i . The kinematic structure of a prismatic joint is used to model the elongation of each cable-driven limb. In order to avoid singularities at the central position of the manipulator at each level, the cable-driven limbs are considered to be crossed. Angular positions of fixed base and moving platform attachment points are given in table I. In this paper, A_i denote the fixed base points of the limbs, B_i denote point of connection of the limbs on the moving platform, L_i denote the limb lengths, and α_i denote the limb angles. The position of the center of the moving platformG,is denoted by $G = [x_G, y_G]$ and the orientation of the manipulator moving platform is denoted by φ with respect to the fixed coordinate frame.

For inverse kinematic analysis, it is assumed that the position and orientation of the moving platform $X = [x, y, \varphi]^T$ is given and the problem is to find the joint variable of the manipulator, $L = [L_1, L_2, L_3, L_4]^T$, $\alpha = [\alpha_1, \alpha_2, \alpha_3, \alpha_4]^T$. For the purpose of analysis and as it is illustrated in figure 2.b, a fixed frame $O : xy$ is attached to the fixed base at the point O, the center of the base point circle which passes through A_is, and another moving coordinate frame G : UV is attached to the manipulator moving platform at point G. Furthermore, assume that the point A_i lie at the radial distance of R_A from point O, and the point B_i lie at the radial distance of R_B from point G in the xy plane, when the manipulator is at central location.

A. Position Analysis

In order to specify the geometry of the manipulator define θ_{Ai}, θ_{Bi} as the absolute angle of the points A_i and B_i at the central configuration of the manipulator, with respect to the fixed frame O. Let's define the instantaneous orientation angle of B_i's as:

$$\varphi_i = \varphi + \theta_{Bi} \tag{1}$$

Therefore, for each limbs, the position of base points given by,

$$A_i = [R_A \cos\theta_{Ai} \ , R_A \ \sin\theta_{Ai}]^T \tag{2}$$

From the geometry of the manipulator as illustrated in figure 2(b), the loop closure equation of each limb, can be written as,

$$\overrightarrow{A_iG} = \overrightarrow{A_iB_i} + \overrightarrow{B_i\,G} \tag{3}$$

By writing the vector loop closure component-wise and some arithmetic operations the limb lengths and the limb angles are uniquely determined.

$$L_i = [(x_G + R_B\cos\varphi_i - x_{Ai})^2 + \ (y_G + R_B\sin\varphi_i - y_{Ai})^2 \tag{4}$$

$$\alpha_i = atan2[(y_G + R_B\sin\varphi_i - y_{Ai}) \, , (x_G + R_B\cos\varphi_i - x_{Ai})] \tag{5}$$

B. Jacobian Analysis

Jacobian analysis plays a vital role in the study of robotic manipulators. Jacobian matrix not only reveals the relation between the joint variable velocities $\dot{L}$ and the moving platform velocities$\dot{X}$, it constructs the transformation needed to find the actuator forces τ from the forces acting on the moving platform F. Jacobian matrix of a parallel manipulator is defined as the transformation matrix that converts the moving platform velocities to the joint variable velocities, i.e.,

$$\dot{\boldsymbol{L}} = \boldsymbol{J_M} \, . \dot{\boldsymbol{X}} \tag{6}$$

In which, $\dot{\boldsymbol{L}} = \left[\dot{L_1} \, , \dot{L_2} \, , \dot{L_3} \, , \dot{L_4} \, \right]^T$ is the 4 × 1 limb velocity vector, and $\dot{\boldsymbol{X}} = [\dot{x} \, , \dot{y} , \dot{\varphi}]^T$ is the 3 × 1 moving platform velocity vector. Therefore, the Jacobian matrix $\boldsymbol{J_M}$ is a nonsquare 4 × 3 matrix. In order to obtain the Jacobian matrix, let us differentiate the vector loop equation (3) with respect to time, considering the vector definitions $\hat{\boldsymbol{S}}_{\boldsymbol{i}}$and $\vec{\boldsymbol{E}}_{\boldsymbol{i}}$ illustrated in figure 4. Hence,

$$v_G + \ \dot{\varphi} \left(\hat{K} \times E_i\right) = \dot{L_i} \, \hat{S_i} \ + \ \dot{\alpha_i} \dot{L_i} \left(\hat{K} \ \times \ \hat{S_i} \ \right) \tag{7}$$

In which, $v_G = [\dot{x} \, , \dot{y}]^T$ is the velocity of the moving platform at point G, and $\hat{K}$ is the unit vector in Z direction of fixed coordinate frame A. In order to obtain expressions for $\dot{L_i}$ and $\dot{\alpha_i}$, dot multiply and cross multiply both sides of equation (7) by $\hat{S_i}$ respectively:

$$\boldsymbol{J_M} = \left[\, S_{ix} \right| \ S_{iy} \left| \, E_{ix}S_{iy} - E_{iy} \, S_{ix} \right]_{i=1}^{4} \tag{8}$$

$$\boldsymbol{J_\alpha} = \frac{1}{L_i} \left[-S_{iy} \right| \ S_{ix} \left| \, E_{ix}S_{ix} + E_{iy}S_{iy} \right] \tag{9}$$

Note that the Jacobian matrix J_M and J_α are non-square 3×4 matrix, since the manipulator is a redundant manipulator. Also, J_α is defined as the matrix relating the vector of moving platform velocities, $\dot{\boldsymbol{X}} = [\dot{x} \, , \dot{y}, \dot{\varphi}]^T$, to the vector of angular velocities of the limbs $\dot{\alpha} = [\dot{\alpha}_1 \, , \dot{\alpha}_2 \, , \dot{\alpha}_3 \, , \dot{\alpha}_4 \,]^T$ as:

$$\dot{\boldsymbol{\alpha}} = \boldsymbol{J_\alpha} \, . \dot{\boldsymbol{X}} \tag{10}$$

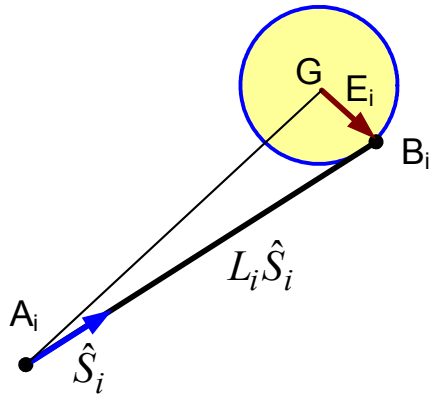

Fig. 3 Vectors definitions for Jacobian derivation of the manipulator.

C. Acceleration Analysis

Acceleration analysis of the limbs and the moving platform is needed for the Dynamic formulation of a parallel manipulator. In acceleration analysis it is intended to derive expressions for the linear and angular accelerations of the limbs, namely $\ddot{L}_i$ and $\ddot{\alpha}_i$ as a function of the moving platform acceleration $\ddot{\boldsymbol{X}} = [\ddot{x}_G \, , \ddot{y}_G \, , \ddot{\varphi}_G]^T$. In order to obtain such relation differentiate the vector loop equation (7) with respect to time, considering the vector definitions $\hat{S}_i$ and $\vec{E}_i$ illustrated in Fig. 3, and noting that $\dot{S}_i = \dot{\alpha}_i\left(\hat{K} \times \hat{S}_i\right)$ and $\dot{\boldsymbol{E}}_{\boldsymbol{i}} = \dot{\varphi}(\hat{\boldsymbol{K}} \times \vec{\boldsymbol{E}}_{\boldsymbol{i}})$. Hence,

$$\begin{aligned} a_G + \ \ddot{\varphi}\left(\hat{K} \times E_i\right) - \dot{\varphi}^2 E_i = \ddot{L}_i\hat{S}_i \\ +2\dot{L}_i\dot{\alpha}_i\left(\hat{K} \times \hat{S}_i\right) + \ddot{\alpha}_i L_i\left(\hat{K} \times \hat{S}_i\right) - \dot{\alpha}_i^2 L_i\hat{S}_i \end{aligned} \tag{11}$$

In order to eliminate $\ddot{\alpha}_i$ and get an expression for $\ddot{L}_i$, dot multiply both side by $\hat{S}_i$ and reorder into,

$$\ddot{L}_i = a_G.\hat{S}_i + \ddot{\varphi}\hat{K}\left(E_i \times \hat{S}_i\right) - \dot{\varphi}^2\left(E_i \, .\hat{S}_i\right) + \dot{\alpha}_i^2 L_i \tag{12}$$

In order to eliminate $\ddot{L}_i$and get an expression for $\ddot{\alpha}_i$, cross multiply both side of (12) by $\ddot{\alpha}_i$:

$$\begin{aligned} \hat{S}_i \times a_G + \ddot{\varphi}\left(E_i \, .\hat{S}_i\right)\hat{K} - \dot{\varphi}^2\left(\hat{S}_i \times E_i\right) = \\ \left(2\dot{L}_i\dot{\alpha}_i + \ddot{\alpha}_i L_i\right)\hat{K} \end{aligned} \tag{13}$$

This simplifies to,

$$\begin{aligned} \ddot{\alpha}_i = \frac{1}{L_i}\left[-S_{iy} \mid S_{ix} \mid E_{ix}S_{ix} + \ E_{iy}S_{iy}\right].\begin{bmatrix} a_{Gx} \\ a_{Gy} \\ \ddot{\varphi} \end{bmatrix} \\ -\frac{1}{L_i}\left(\left(E_{iy}S_{ix} - E_{ix}S_{iy}\right)\dot{\varphi}^2 + 2\dot{L}_i\dot{\alpha}_i\right) \end{aligned} \tag{14}$$

Note that if this equation is written for all four limbs, the first term constitutesJ_α, as defined in equation (10). In order to complete the manipulator acceleration analysis it is necessary to derive expressions for the linear accelerations of the center of mass of each limb. Since in the LAR application, the manipulator is cable driven, it is assumed that the center of mass of each limb is located in the middle of the limbs. Denote the velocity and acceleration of the center of mass of the limbs as v_{Ci} and a_{Ci}, respectively. The velocity of the center of mass is composed as the tangential and normal components as,

$$v_{Ci} = \frac{1}{2}(\dot{L}\hat{S}_i + \dot{\alpha}_i L_i(\hat{K} \times \hat{S}_i) \quad (15)$$

In order to obtain the relation for acceleration of the center of mass of each limb, differentiate (15) with respect to time

$$a_{Ci} = \frac{1}{2}((\ddot{L}_i - \dot{\alpha}_i L_i)\hat{S}_i + (\ddot{\alpha}_i L_i + 2\dot{L}_i\dot{\alpha}_i)(\hat{K} \times \hat{S}_i)) \quad (16)$$

Note that the velocity and acceleration of the center of mass of the limbs v_{Ci} and a_{Ci} are functions of $\dot{L}_i$, $\dot{\alpha}_i$, $\ddot{L}_i$ and $\ddot{\alpha}_i$, whose relation to the manipulator velocity and acceleration $\dot{X}$ and $\ddot{X}$ are given in equations (6),(10), (12) and (14), respectively.

III. Dynamic Analysis

The most popular approach used in the robotics research in order to derive the dynamics equation of motion of a parallel manipulator is the Newton–Euler formulation. In this method the free–body diagrams of the limbs and moving platform are considered and the Newton–Euler equations are applied to each isolated body. Using this approach, all constraint forces and moments between the limbs and the moving platform are obtained. In this paper first the dynamic equation of the manipulator without cable elasticity is derived, and then the dynamic equation of the manipulator with cable elasticity derived and analyzed.

A. Manipulator Dyanamics without cable elasticity model

In order to derive the dynamic equation of manipulator, assumed that the moving platform center of mass is located at the center point G and it has a mass of M and moment of inertia I_M. The inertia parameters of the limbs and moving platform are given in *Table I*. Furthermore, since in the LAR application the manipulator is cable–driven, it is assumed that the mass of the limbs are varying, due to the elongation in the cable length. It is also assumed that the cables are homogeneous, with a circular cross section, and have the density per unit length of ρ_M. The cables are considered to be in a straight line and modeled as rigid bodies, with varying mass of $M_i = \rho_M . L_i$ depending on the cable length. The moment of inertia of the cables are also varying, and can be calculated assuming that they are slender bars with varying length. The moment of inertia of the cables about the fixed point A_i is given by:

$$I_M^{Ai} = \frac{1}{3}ML_i^2 = \frac{\rho_M}{3}L_i^3 \quad (17)$$

The time derivative of mass and moment of inertia of each limb is as following:

$$\dot{M} = \rho_M . \dot{L}_i \;;\; \dot{I}_M^{Ai} = \rho_M L_i^2 \dot{L}_i \quad (18)$$

With these assumptions consider the free-body diagrams of the limbs and the moving platform as illustrated in Fig. 4. The reaction forces at fixed points A_i 's are illustrated componentwise and is denoted by F_{Ai}^N and F_{Ai}^S, in which $\hat{S}$ is along the limb direction and $\hat{N}$ is perpendicular to the limb. Similarly, the internal force at points B_i 's are denoted componentwise as F_{Bi}^N and F_{Bi}^S. The velocity and acceleration of the limb center of mass v_{Ci} and a_{Ci}, are also shown in this figure. Assume that the only external disturbance force and moment existing, acts on the manipulator moving platform, and is denoted by $\boldsymbol{F_D} = [f_{Dx}, f_{Dy}, \tau_D]^T$. Let us first derive the equations of motion of the limbs. The Newton–Euler equations for varying mass system can be written as:

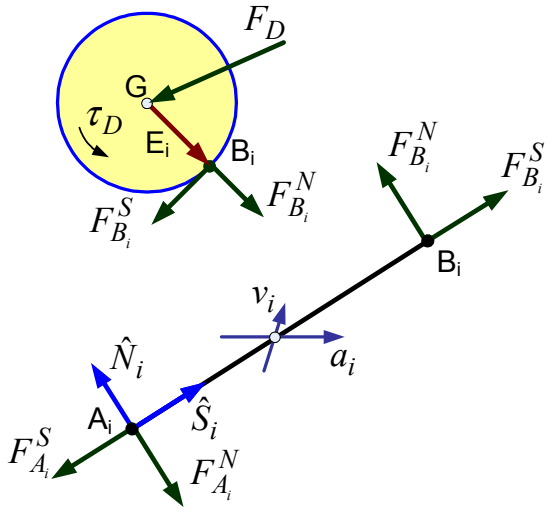

Fig. 4. Free body diagram of manipulator's limb and moving platform

$$\sum \boldsymbol{F_{ext}} = \frac{d}{dt}(M_i\, v_{Ci}) = M_i\, a_{Ci} + \dot{M}\, v_{Ci} \quad (19)$$

$$\sum \boldsymbol{M_{Ai}} = \frac{d}{dt}(I_M^{Ai}\, \dot{\alpha}_i) = I_M^{Ai}\ddot{\alpha}_i + \dot{I}_M^{Ai}\, \dot{\alpha}_i \quad (20)$$

In which, $\sum F_{ext}$ is the summation of all external forces acting on the each limb and $\sum M_{Ai}$ denotes the resulting external moments about the fixed point A_i, and the linear velocity and acceleration of each limb at the center of mass, v_{Ci} and a_{Ci} are given in equations (15)and (16), respectively. Considering the free body diagram of the limb in Fig. 4, the resulting forces and moments can be determined in a vector form as:

$$(F_{Ai}^S - F_{Bi}^S)\,\hat{\boldsymbol{S}} + (F_{Ai}^N - F_{Bi}^N)\,\hat{\boldsymbol{N}} = M_i a_{ci} + \dot{M}_i v_{ci} \quad (21)$$

$$F_{Bi}^N\, L_i = I_M^{Ai}\,\ddot{\alpha}_i + \dot{I}_M^{Ai}\dot{\alpha}_i \quad (22)$$

Substituting v_{Ci} and a_{Ci}, and writing equation (21) componentwise in $\hat{S}$ and $\hat{N}$ direction, with some manipulations this result into:

$$F_{Ai}^S - F_{Bi}^S = \frac{\rho_M}{2}(L_i\ddot{L}_i - (L_i\dot{\alpha}_i)^2 + \dot{L}_i^2) \quad (23)$$

$$F_{Bi}^N - F_{Ai}^N = \frac{\rho_M}{2}(\ddot{\alpha}_i L_i^2 + 3L_i\dot{L}_i\dot{\alpha}_i) \quad (24)$$

$$F_{Bi}^N = \frac{\rho M}{3}(L_i^2\ddot{\alpha}_i + 3L_i\dot{L}_i\dot{\alpha}_i) \quad (25)$$

Furthermore, note that F_{Ai}^S is the actuator forces acting on the limbs. Now, the equation of motion of the moving platform is derived, using the free body diagram depicted in Fig. 4. The Newton-Euler equation of the moving platform is as following:

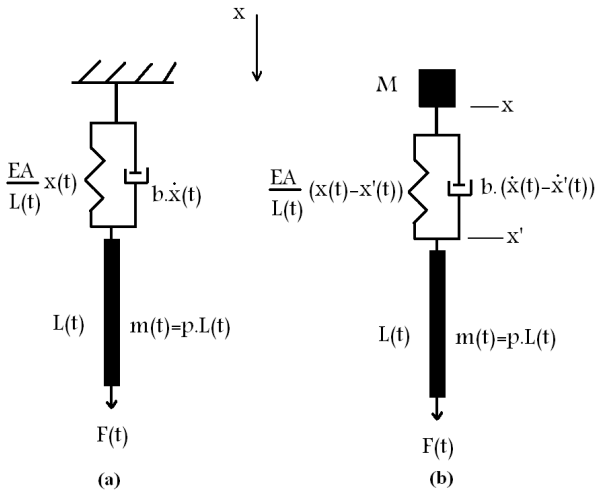

Fig. 5 The schematic of elastic cable modeling

$$\sum \boldsymbol{F_{ext}} = f_D + \sum_{i=1}^{4} \left(F_{Bi}^{S}\,\hat{S}_i + F_{Bi}^{N}\,\hat{N}_i\right) = M\,a_G \tag{26}$$

$$\sum \boldsymbol{M_G} = \tau_D \hat{K} + \sum_{i=1}^{4} \vec{E}_i \times \left(F_{Bi}^{S}\,\hat{S}_i + F_{Bi}^{N}\,\hat{N}_i\right) = I_M \ddot{\varphi}\,\hat{K} \tag{27}$$

Writing the force equation(26) componentwise, with some manipulation:

$$\left\{\begin{array}{l} M\,\ddot{x}_G - f_{Dx} - \sum_{i=1}^{4}\left(F_{Bi}^{S}\,S_x + F_{Bi}^{N}\,S_y\right) = 0 \\ M\,\ddot{y}_G - f_{Dy} - \sum_{i=1}^{4}\left(F_{Bi}^{S}\,S_y + F_{Bi}^{N}\,S_x\right) = 0 \\ I_M\ddot{\varphi} - \tau_D - \sum_{i=1}^{4}\left(F_{Bi}^{S}\left(E_{xi}S_{yi} - E_{yi}S_{xi}\right) + F_{Bi}^{N}\left(E_{xi}S_{xi} - E_{yi}S_{yi}\right)\right) = 0 \end{array}\right\} \tag{28}$$

$$f\left(\boldsymbol{X}, \dot{\boldsymbol{X}}, \ddot{\boldsymbol{X}}, \boldsymbol{\tau_A}, \boldsymbol{F_D}\right) = 0 \tag{29}$$

Equations (28) are the governing equation of motion of the macro manipulator, in which $F_D = \left[f_{Dx}, f_{Dy}, \tau_D\right]^T$ is the disturbance forces/torque exerted on the moving platform, and the interaction forces between the limbs and the moving platform F_{Bi}^{S} and F_{Bi}^{N}, are derived from the limb dynamics and is given in equations (23), and (25), respectively. Furthermore, the vectors $\vec{E}_i$, and $\hat{S}_i$, can be found from inverse kinematic relation by:

$$\vec{E}_i = \left[R_B\cos(\varphi + \theta_{Bi}),\, R_B\sin(\varphi + \theta_{Bi})\right]^T \tag{30}$$

$$\hat{S}_i = \left[\cos\alpha_i,\, \sin\alpha_i\right]^T \tag{31}$$

The first use these equations of are to evaluate the actuator forces τ_A needed to produce a prescribed trajectory $X = [x, y, \varphi]^T$ in presence of the disturbance forces and moments $\boldsymbol{F_D} = \left[f_{Dx}, f_{Dy}, \tau_D\right]^T$. The most important application of these dynamics equations is in the proposed controller strategies for the system. Furthermore, the governing equations of motion of the manipulator can be implemented for dynamic simulation of the system. For dynamic simulation, it is assumed that the actuator forces $\boldsymbol{\tau_A}$, are given and the manipulator motion trajectory $\boldsymbol{X(t)}$, is needed to be determined. Due to implicit nature of the dynamic equation special integration routine capable to integrating implicit differential equations, are used for simulations.

B. Cable Dynamics modelling

The cable modeling is a basic element of theoretical interest in applied mechanics and dynamics. The method to determine the internal forces in cable direction is presented in this section. The tension within the cable elastic behavior, *T*, acts in the cable direction *S*, is modeled by a linear function of the strain within and the axial stiffness of the cable:

$$T = EA\varepsilon \quad ; \quad \varepsilon = \frac{l - l'}{l'} = \frac{\Delta l}{l'} \tag{32}$$

where l' is the unstretched length of the cable, A is the cross section area of the cable element, E is the effective Young's modulus of the cable, and ε is the strain experienced within the cable. The friction between the braids of the cable, along with the polymer coatings creates damping effect. This effect is assumed to be linear with the following relationship between strain rate and damping force. The forces in the cable generated by damping are:

$$F = b.\dot{\Delta l} = b.\left(\dot{l} - \dot{l}'\right) \tag{33}$$

Where, $\dot{\Delta}l$ is the rate of the cable length stretching, and b is the damping coefficient of the cable. In this approach the dynamic equation of cable for Fig. 5. (a),(b) can be written as follows:

For system (a):

$$\begin{gathered} F(t) = \rho_M.L(t).\ddot{\Delta L}(t) + b.\dot{\Delta L} + \frac{EA}{L}\Delta L \\ \Delta L = \Delta x \end{gathered} \tag{34}$$

For system (b):

$$\left\{\begin{array}{l} M.\ddot{x} = \frac{EA}{L}(x - x') + b.(\dot{x} - \dot{x}') \\ F = m\ddot{x} + \frac{EA}{L}(x - x') + b.(\dot{x} - \dot{x}') \end{array}\right\} \tag{35}$$

In which in both cases the cable should be considered to be under tension, or $\Delta L > 0$.

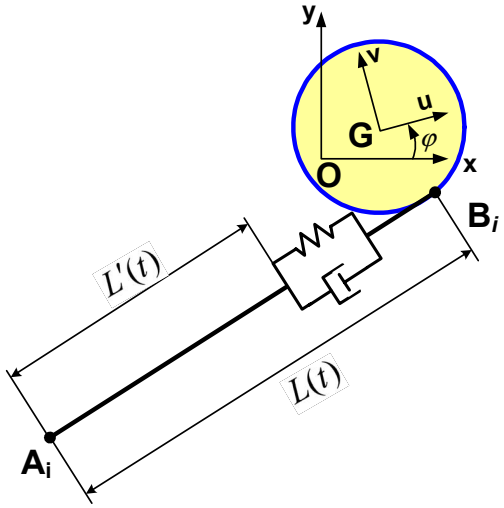

Fig. 6. Manipulator schematic with elastic cables

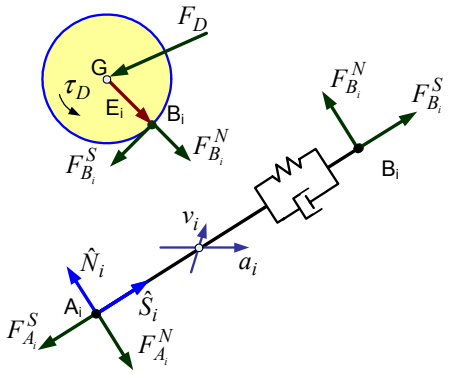

Fig. 7 Free body diagram of manipulator's limb with elastic and damping effects

C. Manipulator Dyanamics with Cable Modelling

Assume that the cables dynamics explained on last section. The overall system is shown in Fig. 6. The free body diagram of manipulator's limb with elasticity and damping effect is shown in Fig. 7. The Newton–Euler formulation is used to rewrite the equations of motion component wise in $\hat{S}$ direction:

$$\begin{Bmatrix} F_{Ai}^S - \frac{\rho_M}{2}\left(L_i\ddot{L}_i - (L_i\dot{\alpha}_i)^2 + \dot{L}_i^2\right) = b\left(\dot{L} - \dot{L}'\right) + \frac{EA}{L}\left(L - L'\right) \\ F_{Bi}^S = b\left(\dot{L} - \dot{L}'\right) + \frac{EA}{L}\left(L - L'\right) \end{Bmatrix} \quad (36)$$

Note that the forces in $\hat{N}$ direction don't change and F_{Ai}^N is obtained from equation (23). Therefore, Equations (28) can be rewritten in an implicit vector form of:

$$\begin{cases} M\,\ddot{x}_G - f_{Dx} - \sum_{i=1}^{4}\left(F_{Bi}^S S_x - F_{Bi}^N S_y\right) = 0 & (37) \\ M\,\ddot{y}_G - f_{Dy} - \sum_{i=1}^{4}\left(F_{Bi}^S S_y + F_{Bi}^N S_x\right) = 0 & (38) \\ I_M\ddot{\varphi} - \tau_D - \sum_{i=1}^{4}\left(F_{Bi}^S\left(E_{xi}S_{yi} - E_{yi}S_{xi}\right) + F_{Bi}^N\left(E_{xi}S_{xi} + E_{yi}S_{yi}\right)\right) = 0 & (39) \\ F - \frac{\rho_M}{2}\left(L_i\ddot{L}_i - (L_i\dot{\alpha}_i)^2 + \dot{L}_i^2\right) - b\left(\dot{L} - \dot{L}'\right) - \frac{EA}{L}\left(L - L'\right) = 0 & (40) \end{cases}$$

$$f\left(\boldsymbol{X}, \dot{\boldsymbol{X}}, \ddot{\boldsymbol{X}}, \boldsymbol{\tau_A}, \boldsymbol{F_D}\right) = 0 \quad (41)$$

In which,

$$\boldsymbol{X} = [\,x, y, \varphi, L'\,]^T \quad ; \quad \boldsymbol{L}' = [L'_1, L'_2, L'_3, L'_4]^T \quad (42)$$

By numerical solution of equation (41), the platform position and orientation $X = [x, y, \varphi]^T$ and the stretched cable length L', is obtained, while L is directly calculated from kinematics position analysis or equation (4).

1) Model Validation and open loop simulation

For open-loop simulations, a proper value for cable elastic and damping coefficient explained in equations (32), (33) must be selected. For this means a reasonable material for cable must be chosen. Casey shows that Plasma is the best option for the LAR system as it has the highest strength-to-weight ratio and also the highest modulus of elasticity apart from steel, [12]. Plasma is the commercial name for an ultra-high density polyethylene based tether manufactured by Cortland Cable, NY. The manufacturer's identified value for elasticity coefficient $E = 38$ GPA, has been chosen for cable modeling and simulations in our analysis. Damping forces in cables tend to be much smaller than the elastic forces, and for this reason, in many cable dynamics studies, damping is neglected. Through various tests that were performed [12], at McGill University a larger range of tether lengths, from 2 m to 25 m are thoroughly studied [13]. The damping coefficient multiplied by the tether length, $b.l \approx 2200\ Ns$ was found to be relatively suitable for the tether lengths that are tested. Another study that Casey has done to arrive to a suitable value for $b.l$, was performed on the actual LAR experimental prototype. Similar instabilities were also observed in the experimental system for high control gains in the close loop, and by verifying the simulation result with, a suitable damping estimate has been reported for the tethers of $b.l = 20000\ Ns$,a value much larger than $b.l = 2200$ Ns which has been found for a vertical tether in [12]. Using the experimentally verified results in [12], the cable parameter that presented in *Table II* is used for the system in the simulations.

As explained before, the most important application of the dynamic equations of the LCM is the direct dynamic simulation of the system. In this case, it is assumed that the actuator forces are given and the manipulator motion is to be determined. Due to implicit nature of the dynamic equation, usual numerical integration routines such as Runge–Kutta methods [9], cannot be used to solve the problem. However, special integration routine [15], which is capable to integrate implicit functions, can be used for dynamic simulations. Simulations are performed to first verify the derived dynamic equations and then to study the behavior of the system. Thus, the model is simulated in some scenarios in which the behavior of the system can be predicted by intuition. In the first simulation, equivalent forces in four directions are applied to the moving platform of the manipulator in its initial condition $X(0) = [\,0.1, 0.1, 0.1]$. This simulation is considered for two cases, once without elastic modeling for cable dynamic, equation (28), and then with elastic effect, equation (37)-(40). As shown in Fig. 8 in both cases the systems oscillates about its equilibrium point $X = [0,0,0]$. This behavior can be easily verified by intuition, since the system is over constrained by elastic cables with low damping coefficient, therefore, the oscillatory output with low decaying ratio is predicted as shown in this figure. Moreover, the strain of the cable along its longitude is relatively large in the elastic model of the cables, generating the growing position errors in the moving. This simulation verifies the importance of elastic modeling of the system to gain more insight of the system dynamics.

In another simulation, the forces are applied only in one direction ($F_1 = 1e3$, $F_2 = 1e3$, $F_3 = 0$, $F_4 = 0$ as in figure 2). The simulation results are given in Fig. 9, which shows a more delayed response for elastic cables compared to that of the manipulator without elasticity.

TABLE II. CABLE ELASTICITY PARAMETERS

Description	Symbol	Quantity
Elasticity coefficient for plasma cable	E	38 GPa
Damping coefficient	b	$\frac{20000}{L}$ Ns/m
Cross section area of the cable	A	4e-4 cm2

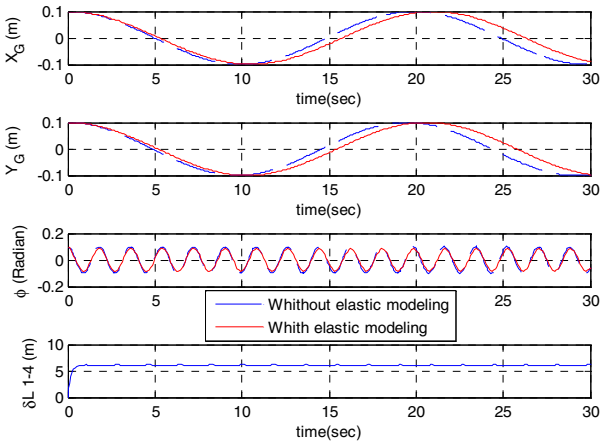

Fig. 8 Oscillating manipulator system while actuated by constant forces and strain of cable elasticity

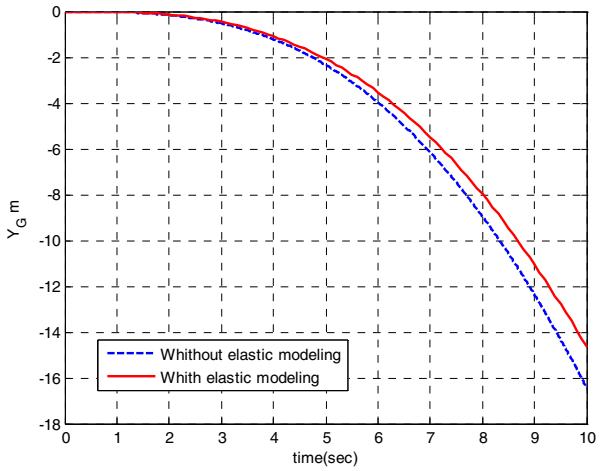

FIG. 9 DISPLACEMENT OF MANIPULATOR IN ONE DIRECTION

IV. CONCLUSIONS

In this paper the kinematic and dynamic analysis of a cable-driven manipulator which is a simplified model of a Large Adaptive Reflector (LAR) is elaborated in detail. In the LAR design the receiver packages are controlled through a large cable driven manipulator (LCM) in 6 DOF. In this paper the simplified 3 DOF cable driven manipulator with one degree of redundancy is analyzed in detail. The kinematic analysis of such manipulator is derived first. Then, the nonlinear dynamic of such mechanism is derived using Newton-Euler formulation. Furthermore, a simple model for cable dynamic that contains elastic and damping effects is proposed. Despite the simplicity of the model, it provides insightful information about the longitude elasticity and damping properties of the cables. Manipulator dynamic with cable elasticity is derived next, and the cable elasticity effects are studied through simulations.

By comparing the simulation results of the manipulator dynamics with and without elasticity effect, a significant difference is observed. Cable elasticity disturbs joint space variables that have been extracted by means of kinematic relations. Moreover, a significant change in the rise time of the system is observed. For a given excitation of actuators, elasticity produces larger delays in the manipulator dynamics, which makes the closed loop control of the manipulator much complicated. This effect is rigorously formulated in the equations (40), which can be explained as a fast pole (dynamics) with high gain added to system dynamics. The effect of this pole can be seen as high forces in high frequencies that makes the control of this system very challenging. Continuing research on suitable control topologies necessary for this system is on the way.

REFERENCES

[1] M.V. Ivashina, A. Van Ardenne, J.D. Bregman, J.G.B. de Vaate, and M. van Veelen. Activities for the square kilometer array (ska) in europe. In Int. Conf. Antenna Theory and Techniques, pages 633–636, Sept.2003.

[2] B. Carlson, L. Bauwens, L. Belototski, E. Cannon, Y. Deng, P. Dewdney, J. Fitzsimmons, D. Halliday, K. Krschner, G. Lachapelle, D. Lo,P. Mousavi, M. Nahon, L. Shafai, S. Stiemer, R. Taylor, and B. Veidt.The large adaptive reflector: A 200-m diameter, wideband, cm-waveradio telescope. In Radio Telescopes-Proc. of SPIE Meeting 4015, pages33–44, Bellingham,WA, 2000.

[3] C. Lambert, A. Saunders, C. Crawford, and M. Nahon. Design of a one-third scale multi-tethered aerostat system for precise positioning of a radio telescope receiver. In CASI Flight Mechanics and OperationsSymposium, Montreal, 2003.

[4] H. Taghirad and M. Nahon, "Dynamic Analysis of A Macro-Micro Redundantly Actuated Parallel Manipulator," to appear in Advanced Robotics, July 2008.

[5] Shiqing Fang, Daniel Franitza, Marc Torlo, Frank Bekes, and Manfred Hiller, Motion Control of a Tendon-Based Parallel Manipulator Using Optimal Tension Distribution, IEEE/ASME Transactions On Mechatronics, Vol. 9, No. 3, 2004.

[6] H. Taghirad and M. Nahon, "Dynamic Analysis of A Macro-Micro Redundantly Actuated Parallel Manipulator," submitted to Robotica, Dec. 2006.

[7] G. Rega, "Nonlinear vibrations of suspended cables, Part I: Modeling and analysis, " Appl. Mech. Rev. 57(6), 443–478, 2004.

[8] G. Rega "Nonlinear dynamics of suspended cables, Part II: Deterministic phenomena, " Appl. Mech. Rev. 57, 479–514, 2004.

[9] L. F. Shampine, Numerical solution of ordinary differential equations. Chapman & Hall, 1994.

[10] C. M. Lambert, "Dynamics Modeling and Conceptual Design of a Multi-tethered Aerostat System, " in Department of Mechanical Engineering. Victoria: University of Victoria, 1999, pp. 158.

[11] C. Lambert, M. Nahon, B. Buckham, M. Seto, and X. Zhao, "Dynamics simulation of a towed underwater vehicle system, part ii: Model validation and turn maneuver optimization," Ocean Engineering, vol. 30, no. 4, pp. 471–485, 2003.

[12] Casey Lambert, Dynamics and control of a multi-tethered aerostat positioning system , PhD thesis, McGill University, 2006.

[13] E. Genho-Hreiche, "Etude de cables soumis a de fortes tensions," Research Project Report, McGill University, 2004.

[14] K. Kozak, Q. Zhou, and J. Wang, "Static Analysis of Cable-Driven Manipulators With Non-Negligible Cable Mass, "IEEE TRANSACTIONS ON ROBOTICS, VOL. 22, NO. 3, JUNE 2006

[15] L. Shampine, "Solving 0=f(t, y(t), y'(t)) in matlab," *Journal of Numerical Mathematics*, vol. 10, no. 4, pp. 291–310, 2002.